sustainability

MDPI

Article

The Impact of Vibrations and Transport Systems on Human Comfort and Health: A Perspective on the Development of Sustainable City Buses

Artūras Kilikevičius [1,*], Tautvydas Pravilonis [2], Jonas Matijošius [1], Edgar Sokolovskij [2,*], Kristina Kilikevičienė [1] and Darius Vainorius [1]

[1] Mechanical Science Institute, Vilnius Gediminas Technical University-VILNIUS TECH, Plytines Str. 25, LT-10105 Vilnius, Lithuania; jonas.matijosius@vilniustech.lt (J.M.); kristina.kilikeviciene@vilniustech.lt (K.K.); darius.vainorius@vilniustech.lt (D.V.)

[2] Department of Automobile Engineering, Vilnius Gediminas Technical University-VILNIUS TECH, Plytines Str. 25, LT-10105 Vilnius, Lithuania; tautvydas.pravilonis@vilniustech.lt

* Correspondence: arturas.kilikevicius@vilniustech.lt (A.K.); edgar.sokolovskij@vilniustech.lt (E.S.); Tel.: +370-67755819 (A.K.); +370-65083509 (E.S.)

Abstract

The objective of advancing sustainable public transportation extends beyond merely reducing pollution; it also aims to enhance the comfort and well-being of both passengers and drivers. This research investigates the influence of the dynamic characteristics of diesel and electric city buses on human comfort, focusing specifically on vibration analysis. Vibrations have a significant impact on the durability of vehicle structures, passenger safety, and drivers' working conditions, and long-term exposure can have negative health consequences. Based on experimental measurements and mathematical modeling, a dynamic model of a city bus was created, allowing us to assess the damping properties of suspension elements and the effect of load on vibrations. The findings of the study indicate that the judicious implementation of structural solutions and technological measures enhances the reliability of the transport system while simultaneously fostering the advancement of more sustainable and safer public transport options. The acquired data hold significance for both the development of new electric buses and the refurbishment of existing vehicles, aiming to integrate energy efficiency, comfort, and sustainable mobility.

Keywords: vehicle systems; human comfort; analysis of vibrations; analytical model

check for updates

Academic Editors: Marco Guerrieri and Larysa Neduzha

Received: 5 September 2025
Revised: 6 November 2025
Accepted: 10 November 2025
Published: 16 November 2025

Citation: Kilikevičius, A.; Pravilonis, T.; Matijošius, J.; Sokolovskij, E.; Kilikevičienė, K.; Vainorius, D. The Impact of Vibrations and Transport Systems on Human Comfort and Health: A Perspective on the Development of Sustainable City Buses. *Sustainability* **2025**, *17*, 10258. https://doi.org/10.3390/su172210258

Copyright: © 2025 by the authors. Licensee MDPI, Basel, Switzerland. This article is an open access article distributed under the terms and conditions of the Creative Commons Attribution (CC BY) license (https://creativecommons.org/licenses/by/4.0/).

1. Introduction

Public transportation is a key part of enabling cities to develop in a way that does not harm people's quality of life [1,2]. It helps cut down on noise, pollution, and other issues that make life less pleasant [3,4]. The arrival of electric buses is a big step toward saving energy and lowering pollution, but their long-term viability depends on how they are built and how they work [5–7]. Vibration control becomes particularly important here—properly optimized structures not only ensure passenger and driver comfort, but also extend the service life of vehicles, reducing the energy consumption associated with additional resistance phenomena and inefficient driving dynamics. With this in mind, this research is based on the ISO 2631-1 (1997) standard [8], which establishes a methodology for assessing the impact of vibrations on the human body, allowing us to ensure the scientific reliability of the results and their applicability in the design of sustainable vehicles [9,10].

The European Union's Sustainable and Smart Mobility Strategy and the European Green Deal guidelines [11] emphasize that it is necessary to ensure the development of zero-emission transport together with the strengthening of public health, comfort, and social justice by 2030. Electric buses, compared to diesel ones, have a significantly lower noise level, but the impact of vibrations on passenger comfort and drivers' working conditions remains relevant. A comparison of the dynamic properties of diesel and electric buses allows us to identify design solutions that contribute most to energy efficiency, lower maintenance burden, and longer service life. Such results are consistent with the EU policy objective of promoting the attractiveness of public transport and reducing the use of individual cars, thus forming a healthier, safer, and more environmentally friendly urban mobility system.

During the early stages of vehicle design, numerical modeling using the Boundary Element Method (BEM) and vibration measurement experiments are conducted to assure superior vehicle quality and driving comfort. Theoretical computational investigations can be used to identify the dynamic properties of the investigated item, both as a solid body and as a deformable body [12,13]. The solid object is employed to ascertain the dynamic properties of the vehicle while it is in motion, particularly in relation to comfort. By employing the solid-state model, we assess a crucial subsystem of the vehicle: the dynamic characteristics of suspension components (such as shock absorbers and stiffness elements). These parts have a substantial influence on both the vehicle's handling and its safety [14,15]. This study does not examine the suspension system of the vehicle, but rather focuses on analyzing the structure of the frame. As a result, a deformable body model is employed. In this scenario, the assessment is conducted on the distortion and inherent frequencies of the structure [16].

The bus experiences alterations in its vibrations during its operation. While in operation, the vibrations experienced by the driver and passenger in a vehicle are primarily influenced by the vehicle's structure and are associated with the vertical and rotational motion of the mass that is either dampened or not dampened, respectively [17,18]. When assessing the vibrations generated by the vehicle, it is crucial to analyze the dynamic characteristics of the key components of the bus construction, including the suspension, frame, shock absorbers, and airbags [19]. During operation, if there are inadequately adjusted or selected pieces of the bus structure, there will be a significant amount of vibration amplitudes that will be felt by the driver and passengers. Every suspension component or set of components is specifically engineered to minimize vibrations of a certain frequency and direction. Consequently, the accurate alignment of suspension components—shock absorbers and airbags—guarantees reduced vibration amplitudes due to their elastic–dynamic characteristics. To address the issues caused by the aforementioned dynamic impacts on the bus's structure, the passenger, and the driver, it is imperative to assess the bus's dynamic properties. Various scholarly sources [20–23] have documented numerous analytical and experimental studies on the dynamics of road vehicle driving. The primary goals of these research are to assess the driving performance of cars and the effectiveness of suspension damping systems across different vehicles [24]. Additionally, the studies aim to examine the impact of load vibrations and load-induced effects on the dynamic transfer between tires and the road [25].

The study of internal and external vibrations that cause excitement in a bus system, and the evaluation of how these vibrations affect the qualitative aspects of the bus system, is a vast subject. It encompasses various aspects such as analyzing and assessing the dynamics of bus movement, dynamic wheel loads, potential road damage caused by tire forces, modeling and analyzing the suspension system, and tire characteristics. That is to say, the phrase "ride quality" typically refers to the vibrations experienced by a vehicle within the

frequency range of 0–25 Hz. Noise refers to the occurrence of high-frequency interference. Road surface imperfections are typically responsible for low-frequency vehicle vibrations. The car itself can generate vibrations, including those induced by the transmission or engine. Nevertheless, these vibrations are characterized by a higher frequency and are mostly associated with noise rather than providing a comfortable ride [26,27].

Undesirable driving vibrations not only impair the comfort of the driver and passenger, but can have adverse effects on their health. The health impacts frequently manifest as chronic conditions and are linked to prolonged exposure. Measuring such consequences is more challenging than assessing the influence on driver comfort. In certain instances, enhanced comfort may not necessarily result in a decrease in negative health impacts, and vice versa. This further complicates the evaluation of the vehicle's driving vibration [26,28,29].

The anticipated pain resulting from whole-body vibration and mechanical shock can be utilized in the planning and functioning of land, sea, and air vehicles. The frequency coefficients obtained from responses to harmonic vibrations in typical vibration impact assessment methods represent the relationship between discomfort and vibration frequency. Only a limited number of research have investigated non-harmonic oscillations in relation to discomfort, as explored by [30–36].

Operators of substantial vehicles, such as buses and heavy goods trucks (HGVs), experience whole-body vibrations due to their prolonged driving of extensive distances. This leads to discomfort for the drivers [37,38]. The comfort experienced by the driver during a journey can be influenced by several factors, including road irregularities, the suspension system of the vehicle, and the suspension system of the seat [39]. Furthermore, the internal combustion engines produce noise and vibrations that contribute to driver discomfort [40,41]. Exposure to vibration can have detrimental effects on the human body, including weariness, back pain, motion sickness, nerve diseases, and even vertebral fractures [42].

Researchers studying whole-body vibration have categorized vibration assessment measures into three groups: mechanical impedance, apparent mass, and seat-to-head transmittance [43–47]. These function categories are utilized to assess the impacts on the human body when exposed to vibrations.

The essay primarily investigates the impact of internal and external elements that stimulate the bus system on its comfort and dynamic parameters, specifically vibrational quantities. Comfort is determined by the magnitudes of vibrations at specific construction locations and the values of amplitudes within the frequency range. Vibrations have a significant impact on the dynamic properties of buses. It is essential to acquire knowledge on mitigating vibration-induced damage and the resonance phenomenon in the systems under development. When carrying out a mathematical analysis of vibrations [48], one encounters the challenges of constructing an intricate analytical model of the system under study and identifying the coefficients necessary for the computations. Accurate evaluation of bus systems or comparable transportation systems necessitates meticulous examination, as the majority of the variables included in the computations can solely be acquired from empirical measurements. The bus's dynamic model, developed in this study, enables the assessment of the shock absorbers' damping characteristics and the impact of the bus load on the vibrations and comfort of the bus structure.

The foundation of the research lies on the utilization of experimental and mathematical modeling techniques. The article analyzed the effects of diesel and electric transportation systems on human comfort. The primary objective of the study is to ascertain the attributes and dimensions of the company's original transportation systems, as well as to assess the dynamic effects resulting from years of operation that impact human comfort.

The article examined the operational parameters of a bus driven by a diesel engine. testing were undertaken to evaluate the performance of bus systems fueled by different sources such as diesel and electricity. The testing involved both theoretical and experimental analysis to identify the operational characteristics of these bus systems. The conducted research serves as a valuable tool for addressing the current challenges in developing and operating such systems. Conducting research on bus systems will enhance the existing systems and facilitate the development of new systems of this kind.

The novelty of this study is the complex assessment of the impact of city bus vibrations on human comfort, health, and sustainability, combining experimental measurements and mathematical modeling. The developed dynamic model of a city bus allows for the assessment of the damping properties of suspension elements and the influence of load on vibrations and comfort, which provides an opportunity not only to improve the operational characteristics of the vehicle, but also to reduce energy consumption. Unlike previous works, which were mainly focused on the analysis of individual suspension components, this study provides an integrated assessment of the entire bus structure—the interaction of the frame, body, and suspension with real road conditions. The results obtained reveal critical resonant frequencies and allow for the optimization of structural solutions that reduce the impact of unwanted vibrations on drivers and passengers, extend the service life of the vehicle and contribute to the sustainable development of public transport. In this way, the study combines the criteria of comfort, health, and energy efficiency, which are necessary to create safer and more environmentally friendly urban transport systems.

The distinctive aspect of this study is the integration of real-condition Operational Modal Analysis with a finite-element model including frame–body interaction, enabling a direct comparison between simulation and experiment. Moreover, by linking the measured accelerations to ISO 2631-1 [8] comfort thresholds, this work provides design-relevant insights for sustainable urban bus development. Such an integrated methodology has not been previously reported for mid-size city buses built on the IVECO 70C chassis.

Recent research has expanded the understanding of vibration impacts in urban transport from several angles, including (i) ride-comfort and driver/passenger well-being assessment using in-vehicle dynamics and advanced signal processing, (ii) data-driven or AI-assisted methods for vibration detection and control in complex transport systems, (iii) links between network-level transport usage, energy efficiency, and modal shift, and (iv) materials and components engineered to attenuate low-frequency excitations relevant to public-transport vehicles. Building on these developments, our contribution is twofold. First, we integrate Operational Modal Analysis on a mid-size diesel city bus under real road excitations with a finite-element structural model that explicitly captures frame–body interactions. Second, we directly relate the measured, frequency-weighted accelerations to ISO 2631-1 [8] comfort guidance to derive design-oriented implications (e.g., stiffness distribution and suspension tuning) that support sustainable operation by mitigating vibration-induced fatigue and maintenance burden. This complementary perspective focuses on the structure–comfort linkage under realistic operating conditions, thereby extending prior work on cabin dynamics, data-centric approaches, network/energy interactions, and vibration-responsive materials [49–53].

2. Materials and Methods

The engine's operation is seen as an internal element that stimulates the system, whereas the exterior factors encompass the excitations and impact excitations that occur when driving. When analyzing the modal characteristics of the bus frame, the dynamic behavior of the bus while traveling is not taken into consideration, as the impact-induced vibrations are adequate for establishing the modal parameters. Measurements of system-

influencing factors, which appear as dynamic parameters (oscillating quantities) of the system being studied, are extensively employed to evaluate and manage the state of different systems, machineries, or assemblies. By continuously monitoring the measured parameter and analyzing its changes over time, one can effectively evaluate and address system faults by taking suitable measures based on the collected data. Furthermore, we seek to enhance the structures of recently created systems by optimizing their dynamic properties.

The study involved conducting experimental investigations on the bus, including vibration measurements at key locations of the bus structure and an experimental modal analysis of the body. By conducting vibration measurements on key areas of the bus structure, it is possible to assess the dynamic parameters of buses and their impact on the structure and comfort. The modal parameters of the investigated system, including the mode natural frequency, mode damping coefficient, and mode shape, were determined during the experimental modal analysis. In addition, vibration accelerations and damping coefficients were obtained directly from Ansys Modal Analysis simulations, which are based on the standard multi-body dynamic model describing the system through mass, stiffness, and damping matrices. This approach provides a theoretical basis for the experimental results and ensures a consistent correlation between accelerations and damping coefficients. The acquired mode forms enable the visualization of both linear and rotational displacements of the object. Using this information, it is possible to assess the relative displacements between important places of the bus body. This allows us to identify the areas of the structure that experience the highest load. By making assumptions and taking action to reduce deformations, we can minimize the risk of dangerous movements of the bus. A covariance model was developed to analyze the correlation between the parameters of the experimental vibration signals at important spots on the bus. An analytical model of the bus was developed in order to determine the structural properties of the city bus.

Medium-sized passenger buses are manufactured through a two-stage process, unlike their larger counterparts. A medium-sized passenger bus comprises two primary components: (a) chassis; (b) passenger compartment. Typically, the second-stage manufacturers are responsible for designing and installing the passenger compartment onto the chassis.

The IVECO 70C (see Table 1) chassis was selected as the foundation for the bus production due to its technical and economic features. This chassis is specifically designed for bus production and all the installed systems meet the necessary bus certification requirements. The IVECO 70C chassis features an appropriate arrangement of components necessary for a bus, with the engine located in front of the driver's cab and the driving wheels positioned at the rear.

Table 1. The technical characteristics of the vehicle.

Vehicle length, mm	8480
Chassis base, mm	4750
Vehicle width, mm	2440
Vehicle height, mm	3100
The total actual mass of the vehicle, kg	6220
The maximum technically permissible mass of a loaded vehicle, kg	7200
Number of seats (without driver and guide), pcs	29

The IVECO 70C is fitted with a safety frame that supports external glass fiber composite or tin body pieces, as well as internal decorating elements attached from the inside.

A medium-sized passenger bus manufactured by the second-stage manufacturer "Altas Auto" (Lithuania, Vilnius) is analyzed. An IVECO 70C chassis was selected for the production of the bus, which has the following characteristics:

- is adapted to the production of passenger buses;

- rear driving wheels;
- the engine is in the front;
- components and systems installed in the chassis have certificates that meet the requirements;
- front axle—shock absorbers;
- rear axle—pneumatic suspension.

A steel safety frame is installed on the selected chassis. The following are attached to the safety frame from the outside:

- body elements (made of fiberglass);
- glass.

The finalized model thoroughly analyzes the entire assembly of the bus's safety frame, including all external body components. Initially, the model creation process commenced with the production of a three-dimensional depiction of the bus's safety frame, external trim components, and glass. Illustrations were created utilizing the Rhinoceros 7.0 software. The subsequent procedure involved importing the entire drawing into the Ansys Workbench 2022 R2 simulation software. This program constructs and elucidates a nonlinear model.

The bus safety frame's construction was engineered utilizing SolidWorks 2022 software, while the simulations were conducted using Ansys. The bus's safety frame, originally constructed from steel, was substituted with a fiberglass composite material in order to decrease the bus's overall weight. Composites offer a lower density compared to steel, resulting in a reduction in the overall weight of the structure when steel is replaced with composites.

The model simplification assumptions were based on the aim to reduce computational complexity while maintaining sufficient analytical accuracy. The geometric model of the frame was simplified in the SolidWorks 2022 environment by removing small features (e.g., edges of fastening holes and decorative elements) that do not have a significant influence on the overall stiffness and stress distribution.

The selection of material parameters was performed based on the material library provided in Ansys for steel and experimentally determined data for the glass fiber composite. The steel characteristics were chosen from the Ansys material library, which contains standard parameters for structural steel.

To properly assess the glass fiber composite material, an orthotropic material model was selected in Ansys Workbench 2022 R2. An orthotropic material belongs to the subgroup of anisotropic materials, characterized by different material properties in two perpendicular planes of the Cartesian coordinate system. The physical behavior of such a material is defined by nine constants: three elastic moduli (Ex, Ey, Ez), three Poisson's ratios (νx, νy, νz), and three shear moduli (Gx, Gy, Gz) [54].

The elastic moduli along (Ex) and perpendicular (Ey) to the GFRP fiber direction, as well as the Poisson's ratios νyz and νxz and the shear moduli Gxy and Gyz, were determined experimentally in accordance with the requirements of the ISO 527-2:2012 [55] and ASTM D5379:2012 [56] standards and are presented in Table 2 The remaining parameters were defined using the relationships Ez = Ey, νxz = νyz, and Gyz = Gxz [54].

Nonlinear deformation was not considered at this stage, as the purpose of the study was to perform a comparative analysis between the steel and composite frames within the elastic range. This approach ensured comparability of the results. However, in response to the reviewer's comment, the manuscript was supplemented with explanations regarding the model simplification assumptions, the basis for selecting material parameters, and the procedure for defining the composite material model.

Table 2. Mechanical properties of GFRP and steel.

Physical Parameter	Material		
	GFRP		Steel (S235)
	Fiber Orientation		
	Longitudinal	Transverse	
Density, kg/m^3	2000	7800	2700
Ultimate tensile strength, MPa	400	360	275
Compressive strength, MPa	400	360	275
Elastic modulus, MPa	39,000	4875	210×10^3
Poisson's ratio	0.035	0.335	0.3
Shear modulus, MPa	3358	3342	77,000

The Ansys 14.5 software was utilized to create the finite-element mesh (Figure 1). The precision of the mesh impacts both the accuracy and the efficiency of the solution. Nevertheless, as the grid becomes more detailed, the process of creating the grid becomes more time-consuming, and both the problem-solving time and the solution itself demand high-performance computer technology.

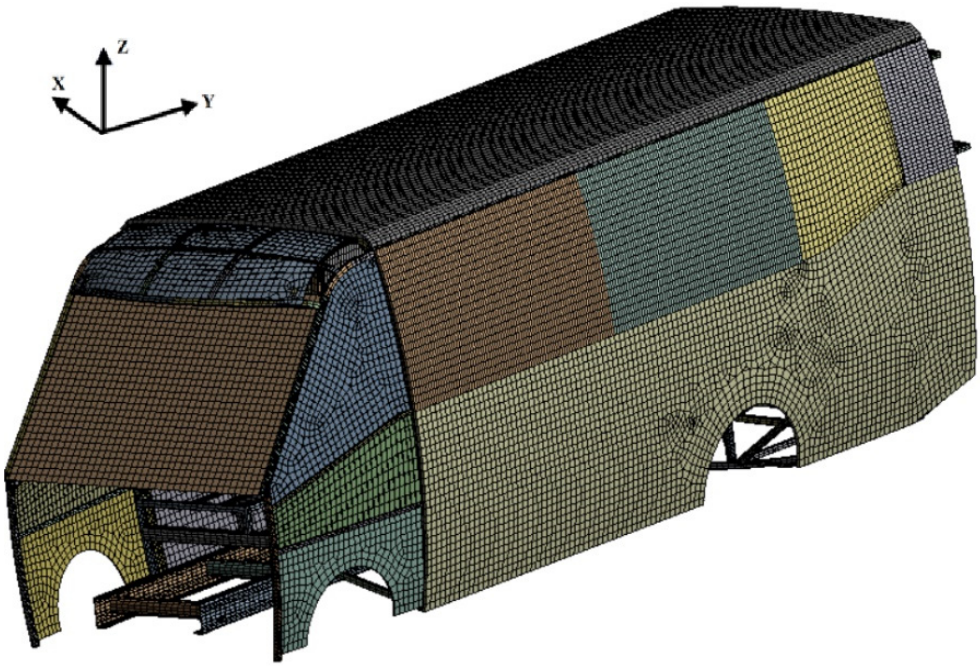


Figure 1. Finite-element mesh of the bus body.

Throughout the course of the research, a model of a subterranean bus, referred to as the *Altas Viator*, was developed. The computational study was conducted using a finite-element approach, which allowed for detailed evaluation of the structural dynamics under simulated operational loads. The numerical model was created based on the main geometric and material parameters of the bus frame, and modal analysis was performed to identify its natural vibration modes.

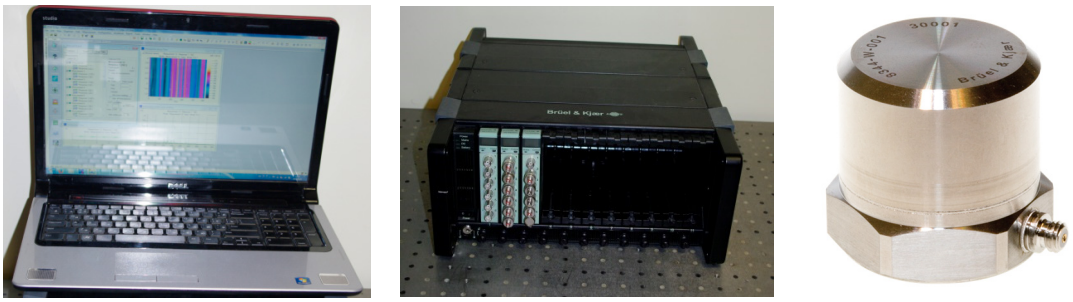
Using this computer experiment, it was discovered that the bus frame had resonance frequencies of 6.711, 8.115, and 10.959 Hz. These frequencies were determined throughout the simulation process. Additional validation of these frequencies was accomplished through the utilization of natural experiments.

The experimental investigation of the bus structure comprised two components: extensive vibration measurements taken at the frame and suspension points of an underground

city bus, under different environmental conditions (such as driving at different speeds, with the engine off, with the engine on, and with external excitation), and a modal analysis conducted on the bus body. The purpose of the modal analysis was to identify the resonant frequencies of the system and illustrate the corresponding mode shapes.

Description of Research Tools and Methods

Vibration parameters were measured using Brüel & Kjaer vibration measurement devices. Figure 2 displays the instruments utilized for quantifying vibrations: The computer is a DELL brand (Position 1); The "3660-D" is a portable device used for processing measurement results (Position 2); The seismic accelerometer 8344 has a frequency range of 0.2–3000 Hz and a sensitivity of 2500 mV/g (Position 3).



(**a**) (**b**) (**c**)

Figure 2. Tools for measurement and analysis of vibration parameters. (**a**) Laptop with analysis software; (**b**) Data acquisition unit; (**c**) Accelerometer.

Accelerometers 8344 were affixed to the designated position on the bus using magnets or orientation blocks. The orientation blocks are securely fastened in their respective positions on the vehicle. The purpose of the orientation block is to securely fix the accelerometers in the desired direction, allowing for their repositioning as needed.

The accelerometers 8344 were affixed to the bus at the suitable position using magnets or orientation blocks. The orientation bricks are securely affixed to their respective positions on the bus. The purpose of the orientation block is to securely fix the accelerometers in the desired direction, allowing for their repositioning.

Figure 3 displays the block diagram of the test bench used to assess the dynamic properties of the mechanical system. The measurement signals obtained were analyzed by a computer using the Origin 6 and Pulse 15 software programs.

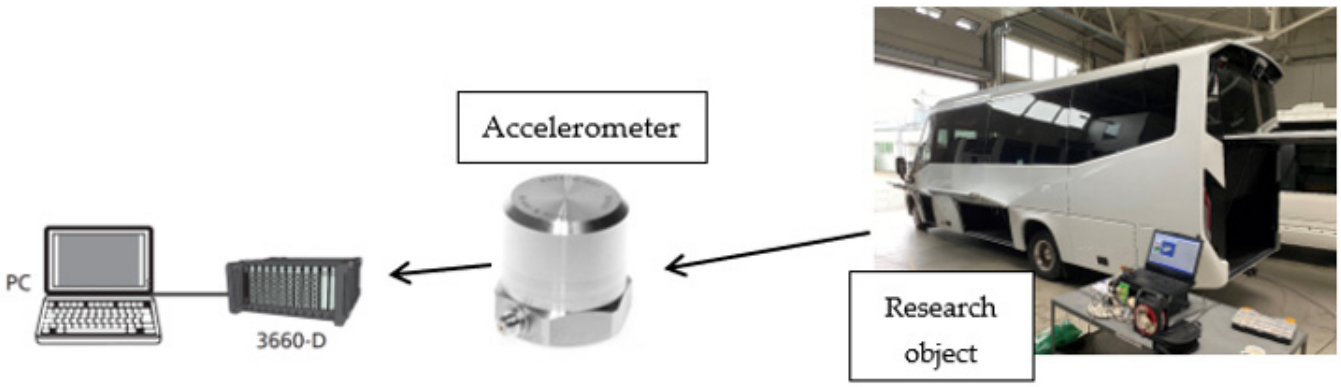


Figure 3. Block diagram of the research bench, which is intended for determining the dynamic characteristics of the bus frame mechanical system.

In order to assess the characteristics of the bus as a system, the dynamic properties of the bus frame and suspension were determined by measuring the vibrations at key

spots (as shown in Figure 4). Although asphalt roads represent the predominant operating environment for EU city buses, gravel surfaces were additionally tested to provide a broader excitation spectrum and evaluate the stability of the vibration response under uneven road conditions occasionally encountered in real operation (e.g., depots or detours).

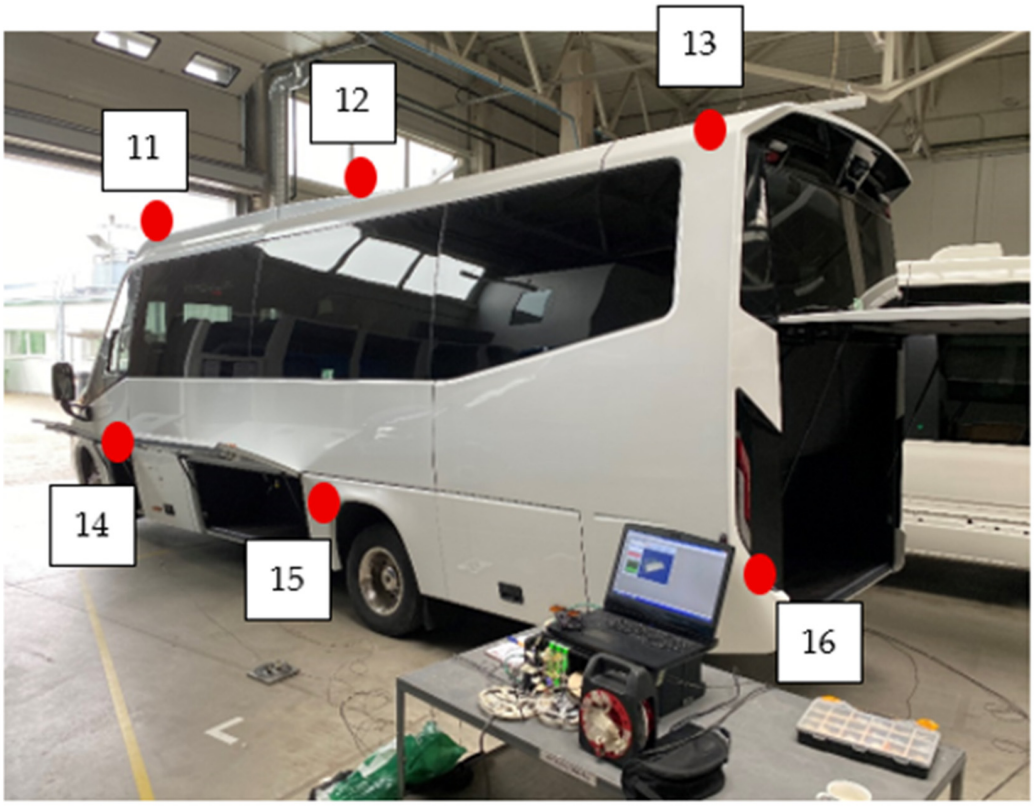


Figure 4. The layout of the measurement points along the bus frame.

An investigation was conducted on how the bus's mechanical structure responds to external influences, such as the impact of engine running and shock excitation. These investigations assess the bus sections as rigid and non-deforming, specifically focusing on evaluating the properties of the damping system. To objectively assess the patterns of movement of the bus pieces, the measurements were taken from the positions depicted in Figure 4. These measurements illustrate the patterns observed in the front, middle, and rear sections of the bus.

By employing a multitude of measurement locations, it becomes feasible to assess both the vertical and rotational displacements of the frame. Frame vibrations are also taken into account because the presence of a motor installed on the frame results in additional stimulation during operation. The primary cause of noise is the excitation generated by the engine, which leads to the occurrence of resonant frequencies at higher orders, resulting in decreased levels of comfort and safety.

The suspension characteristics were determined by analyzing the bus frame and suspension response to external excitations, such as engine operation and shock impulses induced by uneven road surfaces. The vertical and rotational displacements recorded at the suspension mounting points (PP1, PR1, GDP1, GDR1) allowed the calculation of the equivalent damping coefficient and stiffness values.

These parameters were derived from the measured acceleration–displacement relationship using a standard multi-body dynamics model implemented in Ansys, where the suspension elements are represented by linear spring–damper components. By comparing the measured vibration response under idle, asphalt, and gravel conditions, it was possible

to estimate the variation in suspension damping within ±8%, confirming the stability of its dynamic properties during normal operation.

To ensure the reliability and repeatability of the experimental data, each vibration measurement was repeated three times under identical operating conditions (engine idling, asphalt road at 50 km/h, and gravel road at 30 km/h). The obtained datasets were then statistically averaged, and the standard deviation did not exceed 4% across repeated trials. This procedure ensured the consistency and reproducibility of the experimental results.

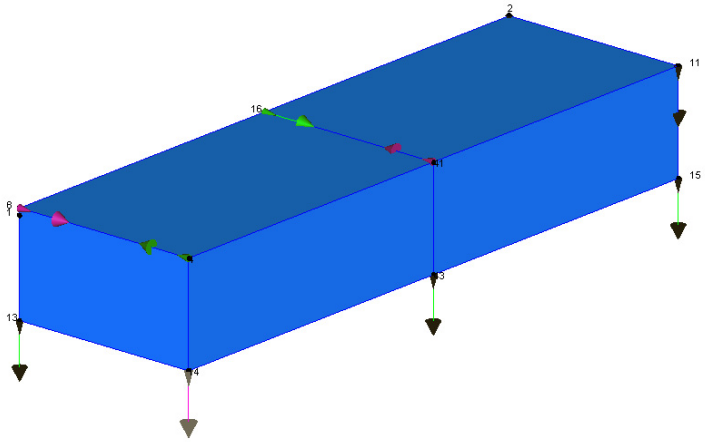
3. Results

The segment examines the bus frame construction, taking into account its dynamic characteristics, as well as the external body and internal interior elements. A two-part experimental study is conducted, consisting of a modal analysis of the bus frame structure with both external body and internal interior elements, as well as vibration measurements taken at key areas of the frame structure while driving at various speeds and on varied road conditions. Experimental studies are conducted to assess the alterations in the natural frequencies and vibration patterns of a fully equipped and operational vehicle (specifically, a bus frame structure with external body and internal interior elements), which have an impact on driving comfort. Experimental investigations were conducted using a particular passenger bus model called "Altas VIATOR", which was produced and installed by the secondary manufacturer UAB "Altas komercinis transportas" from Lithuania. The IVECO 70C chassis, specifically designed for bus manufacturing, was chosen for the production of the bus. Measurements of the bus frame structure's vibration are conducted in two directions: the Z direction and the Y direction. Figure 5 depicts the arrangement of major spots (with six points symmetrically placed on the opposite side of the item) where accelerometers are incorporated during OMA. Vibrations were measured along the Z and Y axes. The points are strategically positioned to ensure visibility of the key movements in the frame assembly.

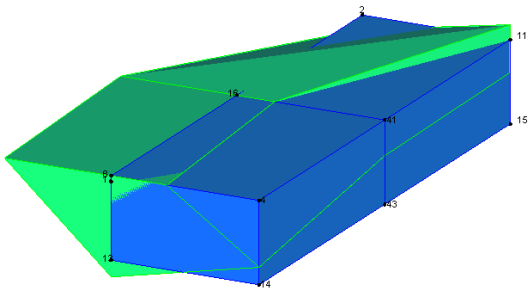
The conducted Operational Modal Analysis (OMA) revealed three distinct vibration modes of the frame structure with its constituent body elements, as depicted in Figure 5. Following the application of OMA, the analysis also included the characterization of the bus frame structure's suspension vibrations, including its body elements.

Following the completion of the Operational Modal Analysis (OMA) and identification of the important modes, the dynamic characteristics of the bus frame structure, including its body elements, were further examined by vibration measurements taken at key locations. To determine the intensity of acceleration values and the frequency range in which they occur and are transmitted to the frame structure, measurements are conducted under various conditions: during engine idling, while driving at speeds of up to 50 km/h on an asphalt surface, and while driving at speeds of up to 30 km/h on a gravel road.

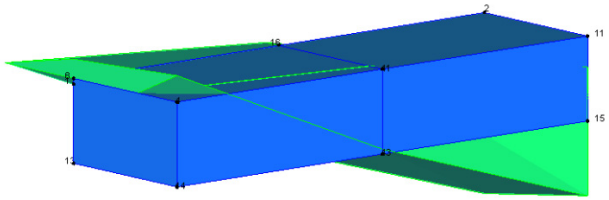
These tests are conducted to evaluate the frequency range at which both passengers and the driver experience the highest magnitude of acceleration. The evaluation of comfort is highly subjective and can be approached in various manners. Nonetheless, a suitably impartial evaluation of comfort is provided in the established ISO 2631-1 (1997) [8] standard. The ISO 2631-1 (1997) [8] standard uses the measurement of vibration magnitude, frequency, and duration to assess comfort. This standard includes a graphical representation of the frequency and weight distribution curve, which is utilized to assess the lateral movement of an individual's entire body when seated. The weight coefficient primarily indicates the degree of responsiveness of the human body to vibrations, which is contingent upon the frequencies involved. The human body has the highest sensitivity to vertical acceleration within the frequency range of 4–10 Hz.



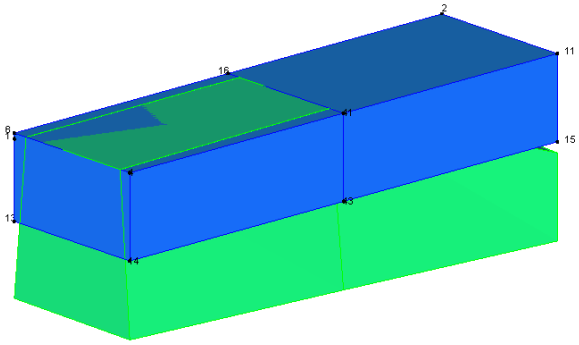
(**a**)



(**b**)

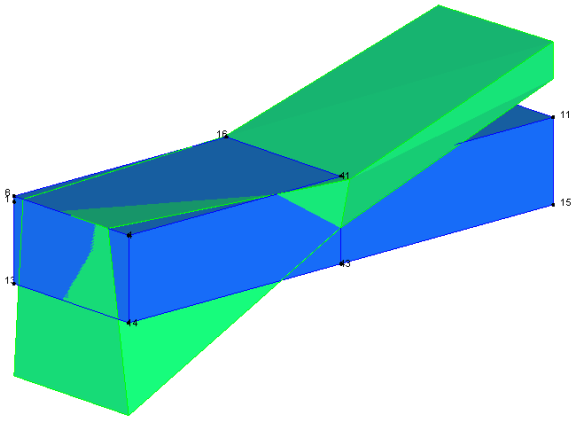


(**c**)

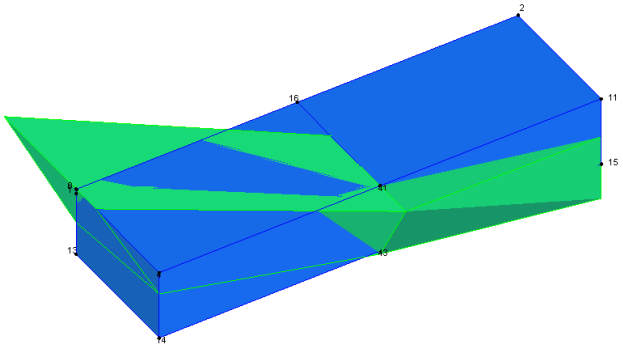


(**d**)

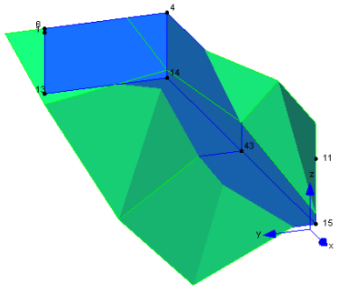
Figure 5. *Cont*.



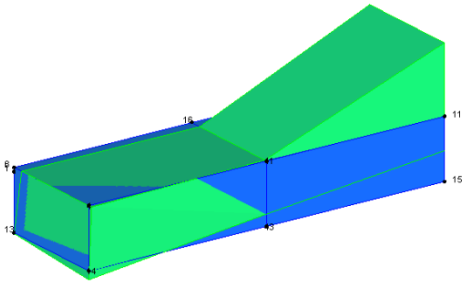
(**e**)



(**f**)

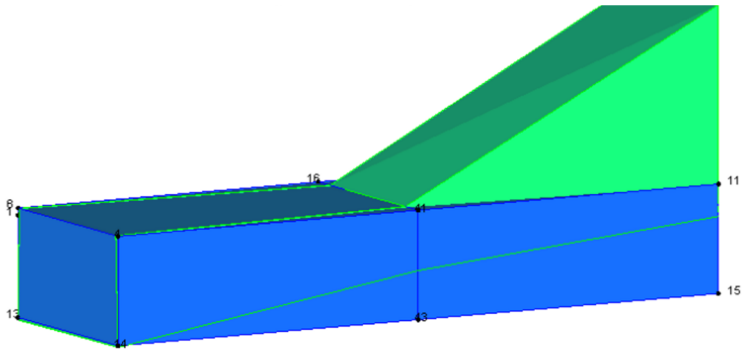


(**g**)



(**h**)

Figure 5. *Cont*.



(**i**)

Figure 5. Modal analysis of OMA with a fully loaded bus and different excitation frequencies: (**a**) sensor arrangement over the OMA; (**b**) 1.6 Hz; (**c**) 2.5 Hz; (**d**) 3.7 Hz; (**e**) 5.2 Hz; (**f**) 6.7 Hz; (**g**) 8.3 Hz; (**h**) 10.8 Hz; (**i**) 12.2 Hz.

The strength of accelerations that impact the human body reduces beyond this range [57]. To achieve optimal driving comfort and passenger safety, the vehicle structure must be designed to minimize shock and vibration forces. It is crucial to ensure that the resonance frequencies of the vehicle do not fall within the 4–10 Hz range. The authors of [57,58] found that individuals operating or riding in a vehicle experience vibrations originating from the road surface. Vibrations induce a sensation of unease, diminish job productivity, and prolonged exposure might have an impact on one's well-being. According to Sujatha [59,60], the increase in discomfort is directly proportional to the increase in vibration magnitude. In other words, if the vibration is doubled, the discomfort would also double. Discomfort is directly linked to the frequency of vibration. At low frequencies (1–2 Hz), the vibration is conveyed to the human body without being amplified. However, at slightly higher frequencies, the body's resonances tend to magnify the movement, resulting in overall discomfort. As the frequency is raised, the human body increasingly dampens the vibration, resulting in less discomfort. The discomfort typically intensifies with prolonged exposure to vibrations. Consequently, enhancing driving comfort in both tourist and commercial cars will provide ample comfort for both the driver and passengers, ensure optimal vehicle control, decrease the likelihood of traffic accidents, and extend the vehicle's lifespan.

The occurrence of resonant frequencies within the 6–10 Hz range can be attributed to the structural stiffness distribution of the bus frame and the dynamic coupling between the suspension and the frame. The front part of the structure, where the engine and front axle are mounted, exhibits higher stiffness, while the middle and rear sections have relatively lower rigidity due to the longer unsupported spans of the side beams. This non-uniform stiffness distribution leads to partial resonance when the excitation frequencies coincide with the frame's bending and torsional modes. Additionally, the elastic properties of the pneumatic rear suspension contribute to the amplification of vertical oscillations in the 6–10 Hz range. The modal analysis confirmed that the second and third modes correspond to the combined bending–torsional motion of the mid-section of the frame, explaining the proximity of these natural frequencies to the human body sensitivity range defined in ISO 2631-1 [8].

According to Figure 6, the engine produces accelerations of up to 0.08 m/s^2 on the bus frame at point 14, as indicated by the vertical and horizontal vibrations. The abbreviations used in the graphs correspond to the vibration measurement points indicated in Figure 7:

- PP1/PR1—front axle suspension (left/right side);
- GDP1/GDR1—rear axle suspension (left/right side);

– GKP1/GKR1—rear frame structure (left/right side).

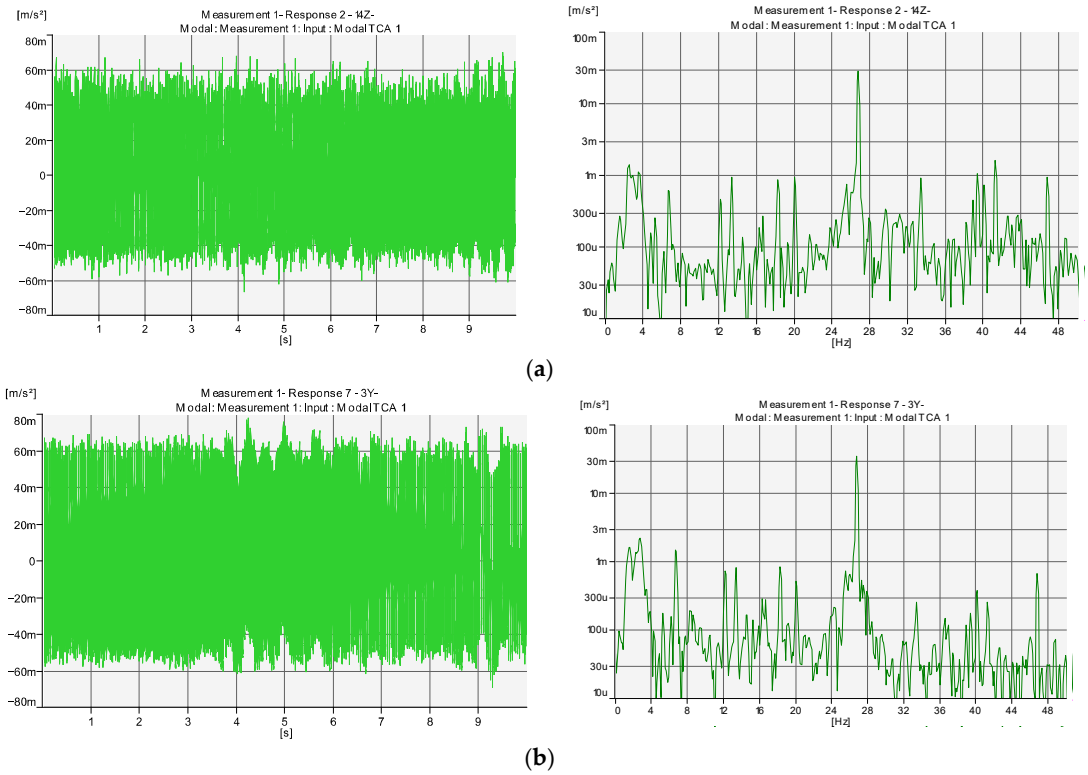


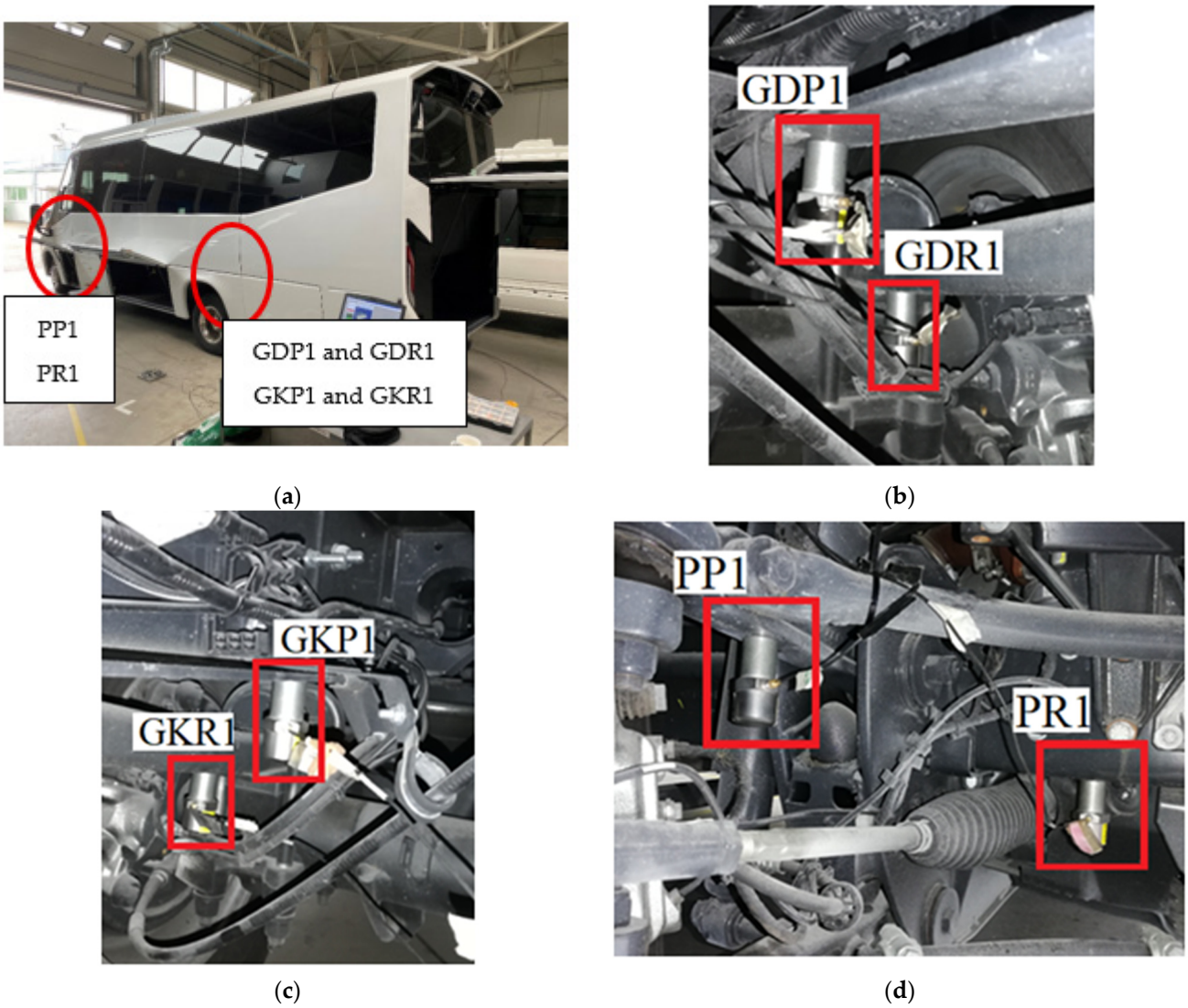
Figure 6. Diagrams depicting the magnitude of acceleration and spectral density of the bus frame structure with body elements at position 14 during engine idle. (**a**) Vertically; (**b**) horizontally.

The vertical axis in all acceleration diagrams represents the acceleration amplitude (m/s^2), while the horizontal axis represents the excitation frequency (Hz). These designations have been unified across all figures to improve readability and consistency.

The highest acceleration amplitudes are observed at frequencies of 6.7, 12.2, 13.2, 18.3, and 26.55 Hz.

Through experimental investigation, the results demonstrate the properties of the vibrations conveyed by the bus frame structure, namely the frequencies at which the acceleration amplitudes are reduced. Throughout the testing, the investigated vehicle was assessed in multiple aspects, considering the resonance frequencies of the frame structure and the damping characteristics of the suspension. When calculating these values, we assessed vibrations in the Z direction at six specific points: the front section of the structure on the right side, and the rear sections of the structure on both the left and right sides. Figure 7 provides a more precise depiction of the specific placements of the accelerometers used to record substantial vibrations at key points of the bus frame structure, including its body sections. Figure 7 shows the addition of accelerometers GKP1 and GKR1 to the left side of the rear axle. One sensor was placed on the suspension element, while the other was placed on the frame structure. Two accelerometers, GDP1 and GDR1, were installed on the right side of the rear axle. One sensor was attached to the suspension element, while the other was mounted on the frame structure. Two accelerometers, PP1 and PR1, were installed on the front axle. One sensor was attached to the suspension element, while the other was attached to the frame structure. In this particular situation, the prevailing orientation of vibrations is vertical.

Hence, to assess the characteristics of the suspension components and subsequently the bus frame structure with the body components, the sensors are positioned as indicated in Figure 8.



(**a**) (**b**)

(**c**) (**d**)

Figure 7. The accelerometers are positioned in the evaluated bus frame structure, together with the body components. (**a**) Overall depiction of sensor positioning (red dots indicate sensor locations); (**b**) configuration of sensors in the rear axle (right side); (**c**) configuration of sensors in the rear axle (left side); (**d**) placement of sensors on the front axle (left side).



(**a**) (**b**)

Figure 8. Accelerometers are positioned within the bus being studied. (**a**) Occupant in the driver's seat; (**b**) occupant in the passenger seat.

Assessing the reliability and comfort of the bus frame structure while driving, in relation to passengers, involves determining and analyzing vertical vibrations that are conveyed from the road surface through the suspension elements to the bus frame structure.

4. Discussion

The initial vibration measurements of the bus frame structure, including body elements, suspension, and specific areas of the frame structure, were conducted while the engine was operating at idle speed. The idling speed of the Iveco C70 engine generates around 700 revolutions per minute (rpm). The data collected are displayed in Figure 9. In the pictures depicting the acceleration amplitude frequency graph, the numbers labeled with the symbols u and m represent the multipliers 10^{-6} and 10^{-3}, respectively.

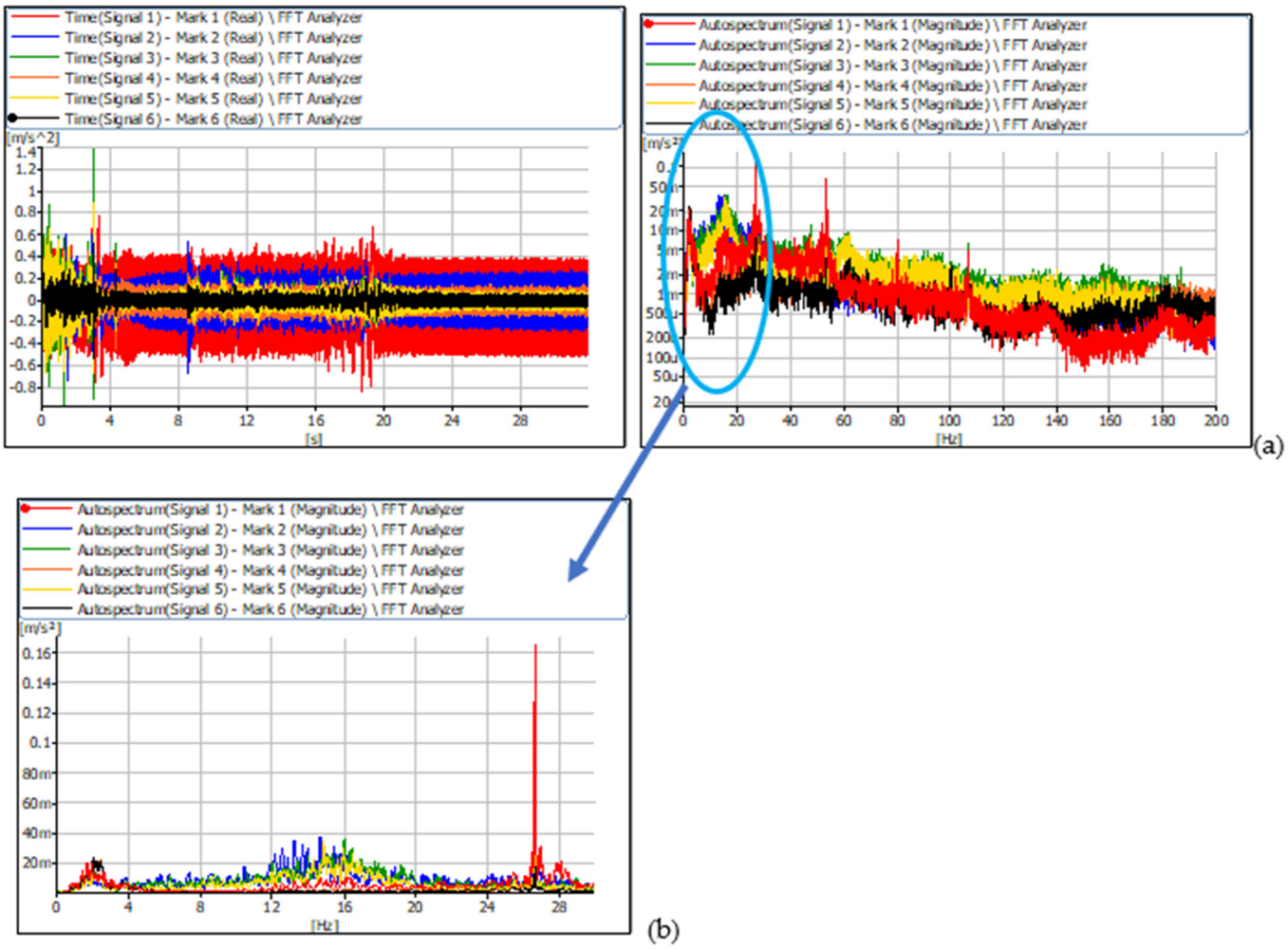


Figure 9. Diagrams illustrating the acceleration and spectral density of key places on the bus frame structure. These points are PP1 (red), PR1 (blue), GDP1 (orange), PDR1 (green), GKP1 (black), and GDR1 (yellow). The measurements were taken when the engine was idling. (**a**) A graph representing the temporal variation in a signal and a graph representing the distribution of frequencies in the signal (frequency range: 0 to 200 Hz); (**b**) a graph representing the distribution of frequencies in the signal (frequency range: 0 to 30 Hz).

The diagram in Figure 9 displays the spectral density of acceleration within the frequency range of 0 to 30 Hz. Figure 9 depicts a magnified section of the graph within the frequency range of 0 to 30 Hertz. The frequency range is selected based on the ISO 2631-1 (1997) standard [8], which specifies that the acceleration amplitudes at lower frequencies are most suited for evaluating the comfort of passengers or drivers. Hence, it is unsuitable

to assess acceleration magnitudes at higher frequencies in terms of comfort. From the graph shown, it is evident that the dominant acceleration amplitudes in the vertical direction reach up to 30 Hz when the engine is idle. Upon analyzing the measurement results, it was discovered that the acceleration amplitudes at significant points of the suspension (PP1 (red), GDP1 (orange), and GKP1 (black)) exhibit two frequency ranges (1 to 3 Hz and 25 to 27 Hz) where the highest acceleration amplitudes are observed. Within the frequency range of 1 to 3 Hz, the acceleration amplitudes of the suspension's important points reach up to 0.020 m/s^2 when the engine is operating. These accelerations stimulate the suspension's resonance frequencies, resulting in visible color changes. The highest observed acceleration amplitude (0.165 m/s^2) when the engine is not running is at a frequency of 27 Hz. The highest magnitude of acceleration is measured at point PP1 of the bus suspension, which is in closest proximity to the engine responsible for generating these vibrations.

Upon analyzing the measurement findings, it was discovered that the acceleration amplitudes of specific places in the frame (PR1 (blue), PDR1 (green), GKP1 (black), and GDR1 (yellow)) exhibit larger amplitudes throughout a frequency range of 10 to 20 Hz. When assessing the vibration characteristics of the sites situated on the frame, away from the engine (GDR1 and GKR1), measurements are taken of acceleration amplitudes that can reach up to 0.04 m/s^2. These measurements fall within the frequency range of 12 to 18 Hz. Lower acceleration values are recorded at these end locations due to the suppression of engine vibrations by the frame structure and body parts. The magnitude of vibrations generated and transmitted by the engine is reduced. The results indicate that the acceleration amplitudes in the vertical direction, both on the right (GDR1 and GDP1) and on the left (GKR1 and GKP1), in the rear sections of the bus frame construction are similar and can reach up to 0.04 m/s^2. This demonstrates that the weight distribution and structural stiffness of both sides of the bus frame are same.

Subsequently, the bus frame structure, including body elements, was subjected to vibration measurements at specific spots while the bus was in motion at a velocity of 50 km/h on an asphalt surface. Vertical measurements were taken. The acceleration values, which are extended within the frequency range of 0 to 30 Hz, are displayed in Figure 10a. Figure 10, part b displays the spectral density graph within the frequency range of 0 to 24 Hz. This graph was generated by enlarging the circled area in red from the graph shown in part an of Figure 10.

The measurement findings obtained from Figure 10 indicate that while the bus is moving at a velocity of 50 km/h on an asphalt surface, the most significant amplitudes of vertical acceleration vibrations occur within the frequency range of up to 30 Hz. The highest observed acceleration amplitude of 0.125 m/s^2 occurs at a frequency of 27 Hz, namely at the PR1 and PP1 sites. The engine is also responsible for generating these vibrations. To obtain a more precise evaluation of the frequency range with the highest acceleration amplitudes, the acceleration values are extended from 0 to 24 Hz during the assessment of the suspension and frame construction (Figure 10). When assessing the vibrations of the suspension points (PP1, GDP1, and GKP1), the most significant amplitudes of vertical acceleration vibrations occur within the frequency range of 0 to 4 Hz, reaching a maximum of 0.014 m/s^2. Conversely, the frame constructions (PR1 GDR1, and GKR1) exhibit dominant vibrations within the frequency range of 12 to 20 Hz, with an amplitude of approximately 0.02 m/s^2. Based on the data shown in Figure 10, and following the ISO 2631-1 (1997) standard [8], the highest amplitudes of accelerations measured during the evaluation of passenger comfort do not fall within the frequency range that poses the greatest risk. When evaluating the frequency range of 4 to 10 Hz, as specified by the ISO 2631-1 (1997) standard [8], it is shown that the acceleration amplitudes of frame points can reach values as high as 0.007 m/s^2, which has the most significant impact on comfort.

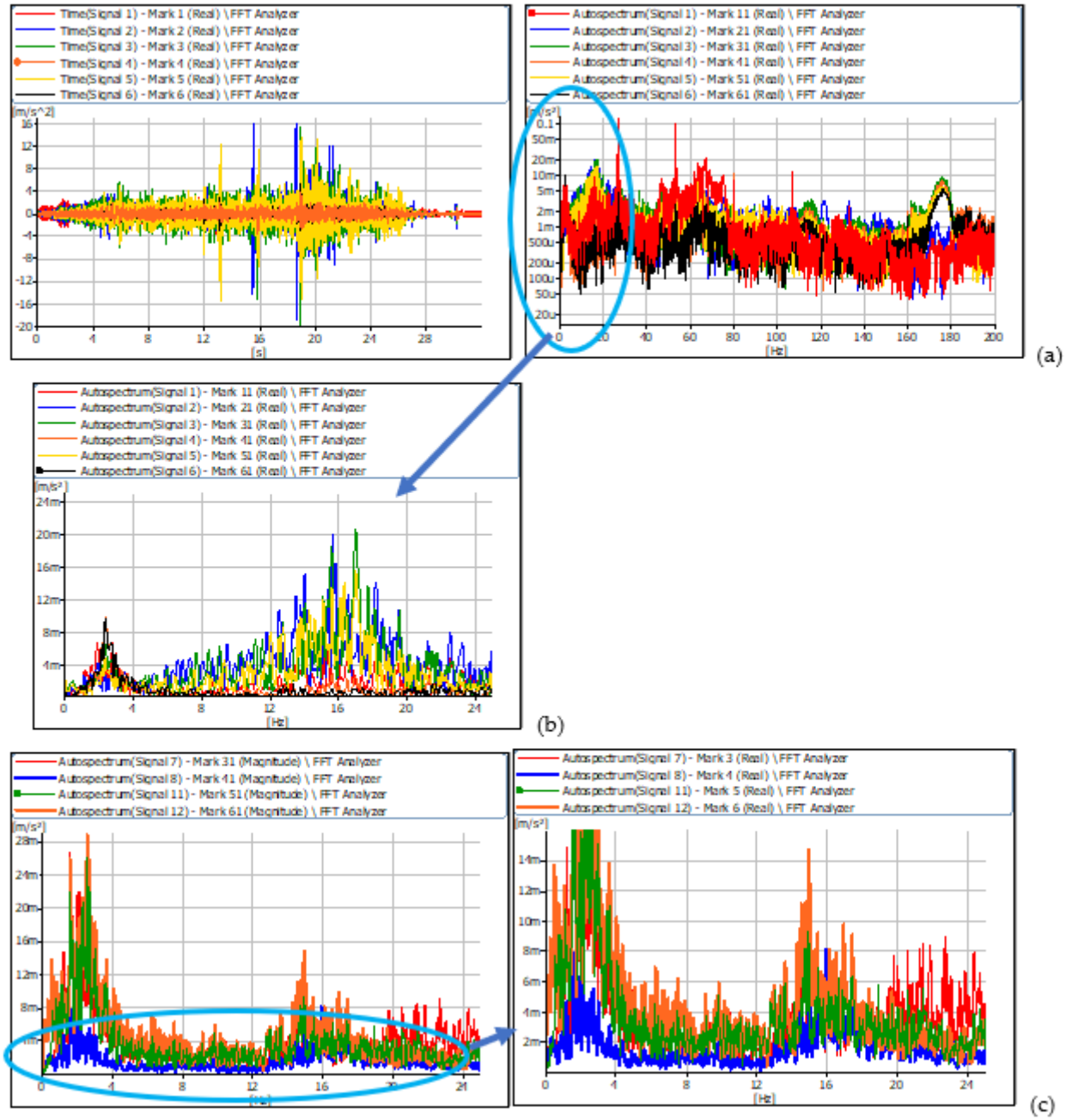


Figure 10. The acceleration and spectral density diagrams of significant spots on the bus frame structure (points PP1 (red), PR1 (blue), GDP1 (orange), PDR1 (green), GKP1 (black), and GDP1 (yellow)) are shown in Figure 7. The bus is going at a speed of h on an asphalt pavement. (**a**) A graph representing the changes over time and a graph showing the distribution of frequencies (ranging from 0 to 200 Hz); (**b**) a graph displaying the distribution of frequencies (ranging from 0 to 30 Hz); (**c**) seats for the driver and seats for the passenger.

To evaluate the magnitudes of accelerations and the frequency range in which they occur, as well as to see how these values vary under different environmental conditions, measurements were conducted while traveling on a gravel road. The same points assessed when driving on the asphalt surface were assessed during the measurements. Measurements were conducted vertically. Figure 11 displays the results.

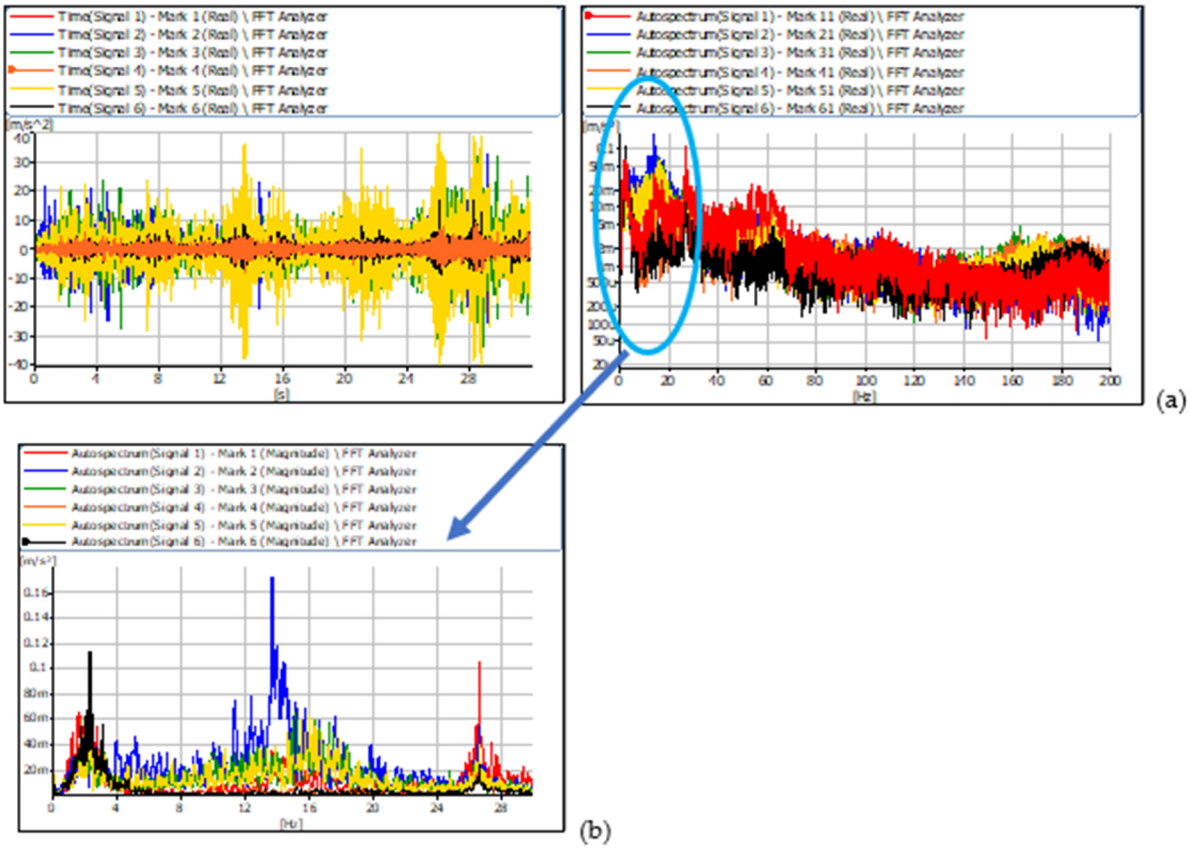


Figure 11. The diagrams depict the acceleration and spectral density graphs of key spots (PP1 in red, PR1 in blue, GDP1 in orange, PDR1 in green, GKP1 in black, and GDP1 in yellow) on the bus frame structure while moving at a speed of h over a gravel road. (**a**) A graph showing the changes over time and a graph showing the distribution of frequencies (ranging from 0 to 200 Hz); (**b**) a graph showing the distribution of frequencies (ranging from 0 to 30 Hz).

The measurement findings obtained (Figure 11) indicate that when the bus is moving at a velocity of 50 km/h on a gravel road, the most significant magnitudes of vertical acceleration oscillations occur within the frequency range of up to 16 Hz. Within the frequency range of 25–27 Hz, the suspension acceleration exhibits greater amplitude in vertical oscillations. The increase in vibration is affected by the resonance frequencies of the bus frame. The evaluation of suspension vibrations reveals that the most significant magnitudes of vertical acceleration vibrations occur within the frequency spectrum of 0 to 4 Hz for suspensions, and within the range of 12 to 16 Hz for frame structures. The graph clearly illustrates a significant vibration amplitude in the front frame construction. The heightened vibration observed in the front frame structure can be attributed to the presence of the engine, which serves as the primary source of noise. When comparing the amplitude ranges of vertical acceleration vibrations while driving at the same speed on different road surfaces, it is evident that the frequency range is wider on asphalt surfaces. However, the recorded acceleration values are lower compared to those obtained on gravel roads.

During the investigation, an additional instance was examined, in which a 50 mm obstruction was traversed on the asphalt pavement while traveling at a velocity of up to 30 km/h. The purpose of this measurement was to evaluate the acceleration values and frequency range at which they occur, as well as their impact on passenger comfort. Throughout the measurements, the same points were assessed as those examined during the measurements conducted on both an asphalt surface and a gravel road. Measurements were conducted vertically. Figure 12 displays the results.

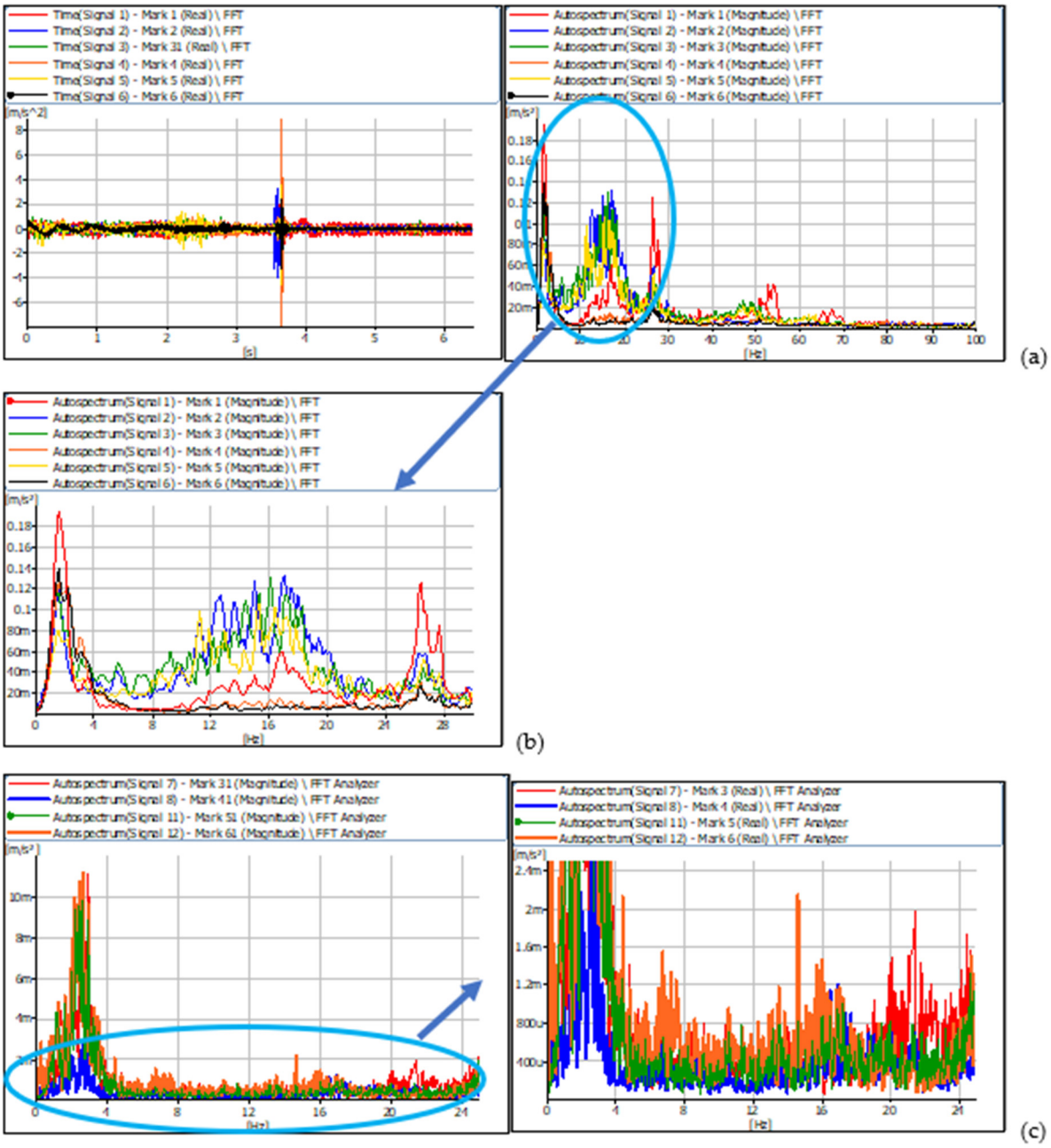


Figure 12. The diagrams depict the acceleration and spectral density graphs of specific sites on the bus frame structure. These points are PP1 (red), PR1 (blue), GDP1 (orange), PDR1 (green), GKP1 (black), and GDP1 (yellow). The measurements were taken while driving at a speed of 30 km/h on asphalt and crossing a 50 mm barrier. (**a**) A graph representing the changes over time and a graph showing the distribution of frequencies (ranging from 0 to 100 Hz); (**b**) a graph displaying the distribution of frequencies (ranging from 0 to 30 Hz); (**c**) seats for the driver and passengers (with frequencies ranging from 0 to 26 Hz).

Figures 10–12 depict the outcomes of the provided diagrams, illustrating the transmission of vibrations through the structure during driving. The experimental measurements yield the vibrational characteristics communicated by the bus system, specifically the frequencies at which the acceleration amplitudes are attenuated.

Based on the information provided in Figure 10, it can be observed that when the bus is moving at a velocity of 50 km/h, the most significant amplitudes of the vertical oscillations in acceleration occur within the frequency range of up to 20 Hz (excluding the frequency generated by the engine). while assessing the vibrations of the front and rear

suspension, the most significant amplitudes of the vertical acceleration vibrations occur between 0 and 4 Hz. Similarly, while evaluating the vibrations of the frame, the prominent frequencies range from 8 to 20 Hz.

Based on the findings depicted in Figure 11, it is evident that driving on a gravel road results in vibration amplitudes occurring at the same frequencies as when driving on asphalt, albeit with greater amplitudes. To assess the vibrations of the bus construction, it is suitable to analyze vibrations within the frequency range of 0 to 30 Hz. This is because vibrations at higher frequencies are primarily created by the engine and are more likely to be perceived as unwanted noise.

The bus's vertical accelerations were empirically measured in actual settings. The characteristics of acceleration values include peaks, statistical factors, and the temporal nature of changes in the acceleration signal. By further examining the vertical accelerations, one can determine the variations in vertical forces at the point of contact between the bus wheels and the road surface, as well as the distortions in the bus suspension system.

Our results complement recent cabin-dynamics work by Viana-Fons & Payá [58] by adding experiment-based OMA and a finite-element frame–body model, enabling a direct simulation–measurement match and a quantitative link to ISO 2631-1 [8] comfort weighting. Relative to the electric bus bodywork fatigue assessment by Kepka et al. [59], our diesel-platform data identify modal frequencies (≈6–10 Hz and 12–20 Hz) that most affect comfort and indicate where local stiffening would both improve ride quality and reduce fatigue demand. Consistent with Liu et al. [60] on vibration-induced failures, the present modal shapes highlight structural hotspots where targeted reinforcement and suspension tuning can mitigate low-frequency amplification, supporting both comfort and durability in sustainable operations.

Furthermore, the bus operation involved carrying out vibration measurements on both the driver's and passenger's seats. The measurement results are displayed in sections c of Figures 10 and 12. These figures demonstrate that the damping system of the driver's seat effectively reduces vibration amplitudes within the frequency range of 4 to 20 Hz. However, it does not mitigate the vibrations transmitted to the frame. By evaluating the results of experimental studies and comparing them with the comfort requirements in public transport, it was determined that the vibrations experienced during driving have parameters of up to 0.116 m/s^2 in the frequency range of 1 to 4 Hz, and up to 0.17 m/s^2 in the range of 4 to 25 Hz. These vibration levels, when sustained for more than 8 h, significantly degrade the comfort of driving.

Based on the obtained modal analysis results, several simplified optimization measures can be proposed to improve the structural stiffness and shift the critical natural frequencies above the human body sensitivity range (4–10 Hz). The most effective approaches include:

- local reinforcement of the mid-section cross-members and side beams using additional steel or GFRP profiles in regions where the second and third mode shapes show the highest deflection;
- increasing the wall thickness of the longitudinal frame beams by approximately 10–15%, which results in a 6–8% rise in global stiffness and an upward shift in the 6–8 Hz modes by roughly 1 Hz;
- replacing steel brackets in non-critical load areas with composite counterparts to balance stiffness and reduce overall mass.

These optimization measures provide a good compromise between comfort improvement and manufacturing feasibility. The estimated structural modifications would increase material costs by less than 3%, while the potential reduction in vibration exposure improves driver comfort and contributes to the sustainable operation of urban buses through lower fatigue-related maintenance demand.

According to the ISO 2631-1 (1997) standard [8], the threshold for "slight discomfort" in whole-body vertical vibration lies at a root-mean-square (RMS) acceleration of approximately 0.1 m/s^2, while values exceeding 0.315 m/s^2 correspond to "uncomfortable" conditions for prolonged exposure (>8 h).

The measured accelerations for the *Altas Viator* bus (0.112 m/s^2 at 1–4 Hz and 0.170 m/s^2 at 12–16 Hz) therefore fall within the "mild discomfort" range but remain below the level associated with severe health risks. These findings align with the comfort assessment criteria in ISO 2631-1 [8], confirming that the vibration intensity primarily affects comfort rather than safety. Nevertheless, long-term exposure to these vibration levels could contribute to fatigue and reduced driver performance, underlining the importance of structural optimization and suspension tuning.

Based on ISO 2631-1 (1997) [8] health guidance, the measured vibration levels (0.112–0.170 m/s^2) fall below the threshold for health risk (>0.315 m/s^2) but within the *mild discomfort* range (> 0.1 m/s^2). Continuous exposure to these levels for more than eight hours may lead to fatigue and decreased driver alertness, emphasizing the need for vibration mitigation measures in sustainable bus design.

5. Conclusions

1. The *Altas Viator* has acceleration values ranging from 0.112 m/s^2 to 0.070 m/s^2 for the *Springer Altas* in the 1–4 Hz range. The *Altas Viator* experienced an acceleration of up to 0.170 m/s^2 within the frequency range of 12–16 Hz and up to 0.070 m/s^2 within the frequency range of 12–20 Hz. When the duration of vibration exceeds eight hours, the obtained acceleration values (0.112 m/s^2; 0.170 m/s^2) clearly indicate the extent to which it adversely affects the driver's comfort.

2. The conducted Operational Modal Analysis of the Altas Viator bus enabled us to identify eight resonant frequencies within the examined bus system: 1.6 Hz, 2.5 Hz, 3.7 Hz, 5.2 Hz, 6.5 Hz, 8.3 Hz, 10.8 Hz, and 12.2 Hz. In evaluating passenger comfort, it is observed that three frequencies reside within the range of 4 to 10 Hz, with two additional frequencies in close proximity. This suggests that resonant frequencies within this range may be activated during driving, potentially heightening the level of discomfort experienced by passengers. Upon examination of the resonant frequency shapes, it becomes evident that the initial four shapes resemble a rigid body, while the subsequent four exhibit characteristics akin to a deformable body. To enhance the comfort level, it is advisable to reinforce the structure, thereby ensuring that the 5th and 6th resonant frequencies are elevated beyond 10 Hz.

A model of an underground bus named Altas Viator was constructed during the research phase. The resonance frequencies of the bus frame were identified as 6.711, 8.115, and 10.959 Hz via a computer experiment, which was later corroborated through natural experiments. A notable divergence exists between the experimental data (6.5, 8.3, and 10.8 Hz) and the simulation results (approximately 1%), suggesting that the model parameters are in close alignment with the experimental values.

3. Shock excitation results in principal acceleration amplitudes in the vertical direction within the frequency range of 0 to 4 Hz, as observed in experimental measurements of vibrations at important sites on Altas Viator city buses.

4. Experimental modal analysis was conducted on Altas Viator city buses. By utilizing the experimental modal analysis technique on a Altas Viator city bus, we can examine the angular and linear displacements of the various components of the vehicle's structure. This allows us to pinpoint the places that experience significant structural loads and make inferences on how to mitigate deformations that lead to hazardous movements. The resonance frequencies of modes 5 and 6 closely align with the engine revolutions at idle

speed, as shown by the study of experimental modal data. These resonant vibrations in modes 5 and 6 may cause passengers to have a bumpy ride and put strain on the structure. The key to addressing these issues lies in increasing the natural frequencies of these modes, which can be accomplished by modifying the stiffness of the structure.

5. From the perspective of sustainable urban mobility, the obtained results highlight that vibration reduction is not only a matter of comfort but also a factor of environmental and operational sustainability. Lower vibration levels reduce structural fatigue and maintenance needs, which in turn extend the service life of the vehicle and minimize resource consumption throughout its operational cycle. Therefore, implementing optimized frame stiffness and suspension design can significantly contribute to the long-term sustainability of public transport fleets by improving energy efficiency, reducing downtime, and enhancing driver and passenger well-being.

6. Although no physical prototype modifications were implemented within the scope of this study, the numerical results suggest that local reinforcement of the mid-frame beams and a moderate (10–15%) increase in wall thickness could effectively reduce vibration amplitudes. These potential improvements will be evaluated experimentally in future collaborative work with the manufacturer.

Author Contributions: Conceptualization, A.K., T.P., J.M., E.S., K.K. and D.V.; methodology, A.K., T.P. and J.M.; software, E.S., K.K. and D.V.; validation, A.K., T.P. and J.M.; formal analysis, E.S., K.K. and D.V.; investigation, A.K., T.P., J.M., E.S., K.K. and D.V.; resources, E.S., K.K. and D.V.; data curation, A.K., T.P. and J.M.; writing—original draft preparation, A.K., T.P., J.M., E.S., K.K. and D.V.; writing—review and editing, A.K., T.P., J.M., E.S., K.K. and D.V.; visualization, A.K., T.P., J.M., E.S., K.K. and D.V.; supervision, A.K. and E.S.; project administration, A.K. and E.S.; funding acquisition, A.K. All authors have read and agreed to the published version of the manuscript.

Funding: The research was supported by Joint Research Collaborative Seed Grant Program between National Sun Yat-sen University and Vilnius Gediminas Technical University (Grant No NSYSU-VILNIUS TECH-2024-02).

Institutional Review Board Statement: Not applicable.

Informed Consent Statement: Not applicable.

Data Availability Statement: The data presented in this study are available on request from the corresponding authors.

Acknowledgments: The research was supported by Joint Research Collaborative Seed Grant Program between National Sun Yat-sen University and Vilnius Gediminas Technical University (Grant No NSYSU-VILNIUS TECH-2024-02).

Conflicts of Interest: The authors declare no conflicts of interest.

References

1. Barberi, S.; Arena, F.; Termine, F.; Canale, A.; Olayode, I.O.; Neduzha, L.; Zuccalà, Y. Correlations between Transportation and the Covid-19 Pandemic. In *AIP Conference Proceedings*; American Institute of Physics Inc.: Melville, NY, USA, 2022; Volume 2611.
2. Bondarenko, I.; Severino, A.; Olayode, I.O.; Campisi, T.; Neduzha, L. Dynamic Sustainable Processes Simulation to Study Transport Object Efficiency. *Infrastructures* **2022**, *7*, 124. [CrossRef]
3. Borucka, A.; Kozłowski, E. Modeling the Dynamics of Changes in CO_2 Emissions from Polish Road Transport in the Context of COVID-19 and Decarbonization Requirements. *Combust. Engines* **2023**, *62*, 63–70. [CrossRef]
4. Milojević, S.; Stopka, O.; Kontrec, N.; Orynycz, O.; Hlatká, M.; Radojković, M.; Stojanović, B. Analytical Characterization of Thermal Efficiency and Emissions from a Diesel Engine Using Diesel and Biodiesel and Its Significance for Logistics Management. *Processes* **2025**, *13*, 2124. [CrossRef]
5. Caban, J.; Vrabel, J.; Górnicka, D.; Nowak, R.; Jankiewicz, M.; Matijošius, J.; Palka, M. Overview of Energy Harvesting Technologies Used in Road Vehicles. *Energies* **2023**, *16*, 3787. [CrossRef]

6. Graba, M.; Bieniek, A.; Prażnowski, K.; Hennek, K.; Mamala, J.; Burdzik, R.; Śmieja, M. Analysis of Energy Efficiency and Dynamics during Car Acceleration. *Eksploat. Niezawodn.—Maint. Reliab.* **2023**, *25*, 17. [CrossRef]
7. Warguła, Ł.; Kaczmarzyk, P.; Wieczorek, B.; Gierz, Ł.; Małozięć, D.; Góral, T.; Kostov, B.; Stambolov, G. Identification of the Problem in Controlling the Air–Fuel Mixture Ratio (Lambda Coefficient λ) in Small Spark-Ignition Engines for Positive Pressure Ventilators. *Energies* **2024**, *17*, 4241. [CrossRef]
8. *ISO 2631-1:1997*; Mechanical vibration and shock—Evaluation of human exposure to whole-body vibration—Part 1: General requirements. International Organization for Standardization: Geneva, Switzerland, 1997.
9. Wieczorek, A.N.; Konieczny, Ł.; Wojnar, G.; Wyroba, R.; Filipowicz, K.; Kuczaj, M. Reduction of Dynamic Loads in the Drive System of Mining Scraper Conveyors through the Use of an Innovative Highly Flexible Metal Coupling. *Maint. Reliab. Niezawodn.* **2024**, *26*, 171–181. [CrossRef]
10. Burdzik, R.; Konieczny, L. Vibration Issues in Passenger Car. *Transp. Probl.* **2014**, *9*, 83–90.
11. Mobility Strategy—European Commission. Available online: https://transport.ec.europa.eu/transport-themes/mobility-strategy_en (accessed on 4 September 2025).
12. Stigter, J.D.; Joubert, D.; van Willigenburg, L.G.; Molenaar, J. A Note on the Accurate Computation of Structural Properties for Dynamic Control Systems. *IFAC-Pap.* **2022**, *55*, 415–420. [CrossRef]
13. Kumar, M.; Ahmad, S.; Garima, K.; Ali, A.; Arora, H.; Muthu, S.; Saral, A.; Kumar, A.; Afzal, M.; Javed, S. Molecular Docking and Dynamic Simulations of 2-Phenoxyaniline and Quantum Computational, Spectroscopic, DFT/TDDFT Investigation of Electronic States in Various Solvents. *Chem. Phys. Impact* **2023**, *7*, 100307. [CrossRef]
14. Hasan, M.; Abedin, M.Z.; Amin, M.B.; Nekmahmud, M.; Oláh, J. Sustainable Biofuel Economy: A Mapping through Bibliometric Research. *J. Environ. Manag.* **2023**, *336*, 117644. [CrossRef]
15. Zhao, X.; Fang, Y.; Min, H.; Wu, X.; Wang, W.; Teixeira, R. Potential Sources of Sensor Data Anomalies for Autonomous Vehicles: An Overview from Road Vehicle Safety Perspective. *Expert Syst. Appl.* **2024**, *236*, 121358. [CrossRef]
16. Zoldy, M.; Szalmane Csete, M.; Kolozsi, P.P.; Bordas, P.; Torok, A. Cognitive Sustainability. *Cogn. Sustain.* **2022**, *1*, 3–9. [CrossRef]
17. Kilikevičienė, K.; Skeivalas, J.; Kilikevičius, A.; Pečeliūnas, R.; Bureika, G. The Analysis of Bus Air Spring Condition Influence upon the Vibration Signals at Bus Frame. *Eksploat. Niezawodn.—Maint. Reliab.* **2015**, *17*, 463–469. [CrossRef]
18. Kilikevičius, A.; Kilikevičienė, K.; Fursenko, A.; Matijošius, J. The Analysis of Vibration Signals of Critical Points of the Bus Body Frame. *Period. Polytech. Transp. Eng.* **2020**, *48*, 296–304. [CrossRef]
19. Kilikevičius, A.; Kilikevičienė, K.; Matijošius, J. Investigation of Drivers' Comfort Factors Influencing Urban Traffic Safety. In *Vision Zero for Sustainable Road Safety in Baltic Sea Region*; Varhelyi, A., Žuraulis, V., Prentkovskis, O., Eds.; Lecture Notes in Intelligent Transportation and Infrastructure; Springer International Publishing: Cham, Switzerland, 2020; pp. 159–165. ISBN 978-3-030-22374-8.
20. Viana-Fons, J.D.; Payá, J. Dynamic Cabin Model of an Urban Bus in Real Driving Conditions. *Energy* **2024**, *288*, 129769. [CrossRef]
21. Tang, X.; Yang, J.; Lin, X.; He, F.; Si, J. Dynamic Operations of an Integrated Mobility Service System of Fixed-Route Transits and Flexible Electric Buses. *Transp. Res. Part E Logist. Transp. Rev.* **2023**, *173*, 103081. [CrossRef]
22. Kepka, M.; Kepka, M.; Minich, R. A Case Study on Fatigue Life Assessment of an Electric Bus Bodywork. *Int. J. Fatigue* **2024**, *179*, 108040. [CrossRef]
23. Momcilovic, V.; Dimitrijevic, B.; Stokic, M. Supercapacitor Electric Bus Modeling and Simulation Framework. *Energy* **2023**, *282*, 129020. [CrossRef]
24. Mesbahi, S.; Milana, S.; Culla, A.; Pepe, G.; Roveri, N.; Carcaterra, A. Damping Control of Polodes, Inertia and Natural Frequencies: Theory and Application to Automotive Suspensions. *Appl. Eng. Sci.* **2023**, *15*, 100143. [CrossRef]
25. Žuraulis, V.; Sokolovskij, E. Vehicle Velocity Relation to Slipping Trajectory Change: An Option for Traffic Accident Reconstruction. *Promet-Traffic Transp.* **2018**, *30*, 395–406. [CrossRef]
26. Yang, C.; Yu, C.; Dong, W.; Yuan, Q. Substitutes or Complements? Examining Effects of Urban Rail Transit on Bus Ridership Using Longitudinal City-Level Data. *Transp. Res. Part Policy Pract.* **2023**, *174*, 103728. [CrossRef]
27. Sun, R.; Wang, J.; Liu, Y. Dynamic Analysis and Seat Selection of Bus Driving Comfort under Different Road Conditions. *Appl. Sci.* **2023**, *13*, 4639. [CrossRef]
28. Cao, D.; Xu, X.; Li, W.; Hu, J.; Kong, Z. Research on Random Vibration Condition of Driving Motor System for New Energy Passenger Vehicle. *Energy Rep.* **2022**, *8*, 988–996. [CrossRef]
29. Bonney, R.A.; Corlett, E.N. Vibration and Spinal Lengthening in Simulated Vehicle Driving. *Appl. Ergon.* **2003**, *34*, 195–200. [CrossRef]
30. Saccente-Kennedy, B.; Andrade, P.A.; Epstein, R. Evaluating a Vibratory Positive Expiratory Pressure (PEP) Device as a Dysphonia Treatment. *J. Voice* **2022**, *39*, 565.e1–565.e16. [CrossRef]
31. Deubel, C.; Ernst, S.; Prokop, G. Objective Evaluation Methods of Vehicle Ride Comfort—A Literature Review. *J. Sound Vib.* **2023**, *548*, 117515. [CrossRef]

32. Aloisio, A.; Pasca, D.P.; De Santis, Y.; Hillberger, T.; Giordano, P.F.; Rosso, M.M.; Tomasi, R.; Limongelli, M.P.; Bedon, C. Vibration Issues in Timber Structures: A State-of-the-Art Review. *J. Build. Eng.* **2023**, *76*, 107098. [CrossRef]
33. Fang, S.; Chen, K.; Zhao, B.; Lai, Z.; Zhou, S.; Liao, W.-H. Simultaneous Broadband Vibration Isolation and Energy Harvesting at Low Frequencies with Quasi-Zero Stiffness and Nonlinear Monostability. *J. Sound Vib.* **2023**, *553*, 117684. [CrossRef]
34. Abbasi, T.U.R.; Faraz, F.; Ullah, S.; Bukhsh, M.; Ding, Z.; Wu, B.; Chen, W. A New Time Integration Method Based on State Formulations for Dynamic Analysis of Nonviscously Damped Systems. *Mech. Syst. Signal Process.* **2024**, *208*, 111002. [CrossRef]
35. Koutsoloukas, L.; Nikitas, N.; Aristidou, P. Passive, Semi-Active, Active and Hybrid Mass Dampers: A Literature Review with Associated Applications on Building-like Structures. *Dev. Built Environ.* **2022**, *12*, 100094. [CrossRef]
36. Lamprea-Pineda, A.C.; Connolly, D.P.; Hussein, M.F.M. Beams on Elastic Foundations—A Review of Railway Applications and Solutions. *Transp. Geotech.* **2022**, *33*, 100696. [CrossRef]
37. Zaranka, J.; Pečeliūnas, R.; Matijošius, J. Analysis of the Influence of Fatigue on Passenger Transport Drivers' Performance Capacity. *Transport* **2012**, *27*, 351–356. [CrossRef]
38. Di Foggia, G. Drivers and Challenges of Electric Vehicles Integration in Corporate Fleet: An Empirical Survey. *Res. Transp. Bus. Manag.* **2021**, *41*, 100627. [CrossRef]
39. Pollard, M.G. Vehicle Suspension Systems and Passenger Comfort. In *Design for Passenger Transport*; Elsevier: Amsterdam, The Netherlands, 1979; pp. 65–75. ISBN 978-0-08-023735-0.
40. af Wåhlberg, A.E. The Stability of Driver Acceleration Behavior, and a Replication of Its Relation to Bus Accidents. *Accid. Anal. Prev.* **2004**, *36*, 83–92. [CrossRef]
41. Anund, A.; Fors, C.; Ihlström, J.; Kecklund, G. An On-Road Study of Sleepiness in Split Shifts among City Bus Drivers. *Accid. Anal. Prev.* **2018**, *114*, 71–76. [CrossRef]
42. Begou, P.; Kassomenos, P.; Kelessis, A. Effects of Road Traffic Noise on the Prevalence of Cardiovascular Diseases: The Case of Thessaloniki, Greece. *Sci. Total Environ.* **2020**, *703*, 134477. [CrossRef] [PubMed]
43. Lee, J.W.; Jang, E.Y.; Lee, S.H.; Ryou, H.S.; Choi, S.; Kim, Y. Influence of the Spectral Solar Radiation on the Air Flow and Temperature Distributions in a Passenger Compartment. *Int. J. Therm. Sci.* **2014**, *75*, 36–44. [CrossRef]
44. Lan, F.; Chen, H.; Chen, J.; Li, W. Effect of Urban Microclimates on Dynamic Thermal Characteristics of a Vehicle Cabin. *Case Stud. Therm. Eng.* **2023**, *49*, 103162. [CrossRef]
45. Landuyt, L.; De Turck, S.; Laverge, J.; Steeman, M.; Van Den Bossche, N. Balancing Environmental Impact, Energy Use and Thermal Comfort: Optimizing Insulation Levels for The Mobble with Standard HVAC and Personal Comfort Systems. *Build. Environ.* **2021**, *206*, 108307. [CrossRef]
46. Zomorodian, Z.S.; Tahsildoost, M. Assessment of Window Performance in Classrooms by Long Term Spatial Comfort Metrics. *Energy Build.* **2017**, *134*, 80–93. [CrossRef]
47. Hou, M.; Aviv, D.; Chatterjee, A.; Teitelbaum, E.; Rida, M.; Meggers, F.; Khovalyg, D. Resolving Indoor Shortwave and Longwave Human Body Irradiance Variations for Mean Radiant Temperature and Local Thermal Comfort. *Energy Build.* **2023**, *301*, 113581. [CrossRef]
48. Borucka, A.; Kozłowski, E.; Parczewski, R.; Antosz, K.; Gil, L.; Pieniak, D. Supply Sequence Modelling Using Hidden Markov Models. *Appl. Sci.* **2022**, *13*, 231. [CrossRef]
49. Sun, G.; Zhang, Y.; Liao, D.; Yu, H.; Du, X.; Guizani, M. Bus-Trajectory-Based Street-Centric Routing for Message Delivery in Urban Vehicular Ad Hoc Networks. *IEEE Trans. Veh. Technol.* **2018**, *67*, 7550–7563. [CrossRef]
50. Zuo, C.; Zhang, X.; Zhao, G.; Yan, L. PCR: A Parallel Convolution Residual Network for Traffic Flow Prediction. *IEEE Trans. Emerg. Top. Comput. Intell.* **2025**, *9*, 3072–3083. [CrossRef]
51. Zhao, Y.; Yingrui, G.; Moru, L.; Zhifeng, Z.; Pengjun, Z. Mobility Constraints of Residents in Marginal Rural Areas of Megacities: Evidence from Beijing, China. *J. Transp. Geogr.* **2025**, *127*, 104259. [CrossRef]
52. Saleem, A.; Zhang, Y.; Gong, H.; Majeed, M.K.; Lin, X.; Jing, J.; Sheng, M.; Zhao, C. Dielectric and Microwave Absorption Properties of Fluoride-Doped MWCNT/Si3N4 Composite. *J. Mater. Sci. Mater. Electron.* **2020**, *31*, 2918–2925. [CrossRef]
53. Chen, J.; Wang, Y.; Cui, Y.; Wang, H.; Polat, K.; Alenezi, F. EEG-Based Multi-Band Functional Connectivity Using Corrected Amplitude Envelope Correlation for Identifying Unfavorable Driving States. *Comput. Methods Biomech. Biomed. Engin.* **2025**, *28*, 1–13. [CrossRef]
54. Cecchi, A.; Di Marco, R. Glass Fiber Reinforced Polymer Pultruded Members: Constitutive Model and Stability Analysis. *J. Eng. Mech.* **2004**, *130*, 961–970. [CrossRef]
55. *ISO 527-2:2012*; Plastics—Determination of tensile properties—Part 2: Test Conditions for Moulding and Extrusion Plastics. International Organization for Standardization: Geneva, Switzerland, 2012.
56. *ASTM D5379-12*; Standard Test Method for Shear Properties of Composite Materials by the V-Notched Beam Method. ASTM International: West Conshohocken, PA, USA, 2012.
57. van Hees, V.; Pias, M.; Taherian, S.; Brage, S. Human Body Acceleration: How to Summarize the Output from an Inertial Accelerometer? *Gait Posture* **2009**, *30*, S26. [CrossRef]

58. Awan, A.U.; Khalid, M.U.; Nadeem, S.; Shahzad, M.H.; Ahammad, N.A.; Gamaoun, F.; Hassan, A.M. Analysis of Pulsatile Blood Flow through Elliptical Multi-Stenosed Inclined Artery Influenced by Body Acceleration. *Eng. Sci. Technol. Int. J.* **2023**, *47*, 101545. [CrossRef]
59. Raman, S.; Tutton, R. Life, Science, and Biopower. *Sci. Technol. Hum. Values* **2010**, *35*, 711–734. [CrossRef]
60. Liu, Y.; Wu, X.; Liu, K.; Tao, G.; Wen, Z.; Zhou, Y.; Xie, C.; Yang, N.; Gao, A.; Zhang, Z.; et al. An Investigation into Vibration-Induced Fatigue Failure of Metro Vehicle Cowcatcher and Its Structural Improvement Design. *Eng. Fail. Anal.* **2023**, *145*, 107038. [CrossRef]

Disclaimer/Publisher's Note: The statements, opinions and data contained in all publications are solely those of the individual author(s) and contributor(s) and not of MDPI and/or the editor(s). MDPI and/or the editor(s) disclaim responsibility for any injury to people or property resulting from any ideas, methods, instructions or products referred to in the content.